J. Membrane Biol. 83, 261–272 (1985)

The Journal of
Membrane Biology

K^+ and Cl^- Conductances in the Apical Membrane from Secreting Oxyntic Cells are Concurrently Inhibited by Divalent Cations

J. Mario Wolosin and John G. Forte
Department of Physiology-Anatomy, University of California, Berkeley, California 94720

Summary. This study concerns the properties of rapid K^+ and Cl transport pathways that are present in the (H^+ + K^+)-ATPase membrane from stimulated, and secreting, gastric oxyntic cells. Ion permeabilities in the isolated stimulation-associated vesicles were monitored via the rates of H^+ efflux under conditions of exclusive H^+/K^+ counterflux or H^+ − Cl co-efflux, as well as by comparison of equilibration rates for ^{86}Rb and ^{36}Cl under conditions of equilibrium exchange and unidirectional salt flux. These latter studies suggest that Rb^+ and Cl pathways are conductive and independent. In spite of the functional independence of the ion pathways, several divalent cations inhibit Rb^+ and Cl isotopic exchange as well as the H^+ efflux that is dependent on either K^+ or anion (Cl , SCN , NO_3) fluxes. Zn^{2+} is the more potent inhibitor, reducing by 50% the sensitive component of K^+, Cl , and NO_3 fluxes at about 20 μM; Mn^{2+} has a similar effect at 200 μM. Ni^{2+} and Co^{2+} were roughly equipotent to Mn^{2+} while Mg^{2+} and Ca^{2+} had no inhibitory effect. These results suggest that the stimulation-induced permeabilities, while functioning independently, may be physically linked, i.e., residing within a single entity. In similar studies carried out in (H^+ + K^+)-ATPase vesicles obtained from nonstimulated cells, no vestiges of sensitivity to the inhibitory divalent cations could be detected. The implications of these findings for the physiology of the oxyntic cell in the context of a model for membrane fusion are discussed.

Key Words K^+ and Cl^- channels · ion transport · gastric secretion · apical membranes · (H^+ + K^+)-ATPase · oxyntic cell stimulation

Introduction

Gastric HCl is generated at the luminal surface of the oxyntic cell (Bradford & Davies, 1950; Dibona, Ito, Berglindh & Sachs, 1979). Large morphological changes are observed at the apical aspect of this cell during transitions between secretory and nonsecretory state (Ito & Schofield, 1974). It has been proposed that these changes are the result of massive fusion of intracellular tubular- and vesicular-shaped membranes with a permanent apical membrane of the resting cell during stimulation, and tubulovesicle recycling from the expanded apical membrane of secreting cells during return to the resting state (Forte, Machen & Forte, 1977).

Studies with isolated membrane fractions have proven to be an invaluable tool to elucidate molecular aspects of the secretory process. An electroneutral (H^+ + K^+)-ATPase, identified in the microsomal fraction of several species, has been widely accepted as the protonmotive source of HCl secretion (Sachs et al., 1976; Forte & Lee, 1977). More recently, we have demonstrated that the changes in cell secretory state are reflected in changes in the structural and functional properties of the ATPase membrane and have defined two inside-out (H^+ + K^+)-ATPase-rich membrane types, the gastric microsomes derived from the tubulovesicles of resting cell, and the stimulation-associated (s.a.) vesicles derived from the expanded apical membrane of the secreting cell (Wolosin & Forte, 1981*a*). Comparative studies of acid accumulation and ion transport in both vesicular types demonstrate that cell stimulation triggers rapid K^+ and Cl^- permeability pathways in the (H^+ + K^+)-ATPase membrane (Wolosin & Forte, 1981*b*, 1984). Similar K^+ and Cl^- permeability increases have been reported in a variety of cells in response to hypotonic solutions generating volume regulatory decrease by KCl loss (Grinstein, Clarke, Rothstein & Gelfand, 1983; Hoffman, Simonsen & Lambert, 1984). In the oxyntic cell the permeability increase is directed to allow efficient HCl generation by combined KCl leak followed by ATPase driven H^+ for K^+ exchange. We report now the effect of divalent cations on the ion permeabilities in s.a. vesicles and gastric microsomes. Implications for the relationships between the ionic pathways and transport regulation in the oxyntic cell are discussed.

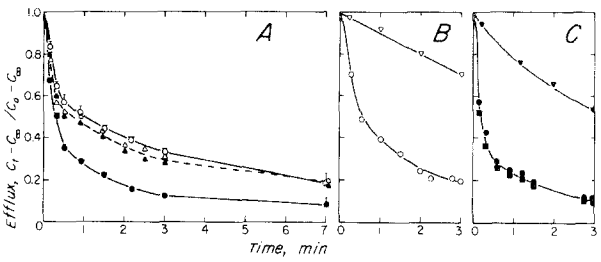

Fig. 1. Features of isotopic flux in s.a. vesicles. (*A*): Efflux of ^{86}Rb and ^{36}Cl under conditions of equilibrium exchange and unidirectional flux. Concentrated vesicle suspensions were pre-equilibrated as described in Materials and Methods with a solution containing 75 mM RbCl double labeled with ^{86}Rb and ^{36}Cl. Isotopic efflux was started by dilution with 19 volumes of unlabeled solution: for equilibrium exchange of Rb (●) and Cl (○), the diluting solution contained 75 mM RbCl; for unidirectional efflux of Rb (▲) and Cl (△), the RbCl in the diluting solution was replaced by 150 mM sucrose. The bars represent variance for duplicate experiments. (*B*): ^{36}Cl efflux in the absence of K^+. Vesicles were pre-equilibrated in a solution containing 75 mM choline Cl labeled with ^{36}Cl. Efflux under equilibrium exchange was measured after dilution in unlabeled with choline Cl solution (○). For unidirectional ^{36}Cl efflux (▽), 150 mM sucrose replaced choline Cl in the diluting solution. (*C*): ^{86}Rb efflux in the absence of Cl. For ^{86}Rb exchange efflux, vesicles pre-equilibrated in ^{86}Rb methane sulfate were diluted in unlabeled solution with (■) or without (●) 50 μM vanadate. For unidirectional efflux (▼), 150 mM sucrose replaced Rb methane sulfonate in the diluting solution. Results are presented as the fraction of exchangeable counts remaining in the vesicles at a given time after the start of isotopic efflux. C_∞ was determined at t = 120 min

Materials and Methods

$(H^+ + K^+)$-ATPase-Rich Vesicles

Stimulation-associated vesicles and gastric microsomes were prepared from stimulated or resting gastric mucosae, respectively, as described elsewhere (Wolosin & Forte, 1981*b*). Ouabain-insensitive K^+-*p*NPPase (*p*-nitrophenylphosphatase) activities were 26 ± 4 μeq/mg · hr for 4 of the s.a. vesicle preparations used and 37 μeq/mg · hr for the gastric microsomal preparations shown.

Radioisotopic Efflux Studies

Concentrated, freshly prepared vesicle suspensions (~5 mg protein/ml) were incubated overnight at 0°C in 150 mM sucrose, 5 mM N-Tris [hydroxymethyl] amino methane-N-tris[hydroxymethyl] methyl-2-amino-methane sulfonate (Tris-TES), 0.02 mM ethylenedinitrilotetraacetic acid (EDTA), 1 mM mercaptoethanol, and 75 mM of either RbCl, choline Cl, Rb methane sulfonate, or NaCl, pH 7.25. After addition of radioisotopes (^{36}Cl, ^{86}Rb, ^{22}Na) and further incubation for 2 hr, the suspensions were diluted under vigorous mixing with 18-19 volumes of the desired efflux solution at room temperature (23–25°C). For equilibrium exchange experiments unlabeled solution identical to the incubation solution was used. For unidirectional fluxes, the 75 mM, salt was replaced by 150 mM sucrose. Aliquots (100–150 μl) were withdrawn at intervals and placed on the center of Gelman GN-6 (0.45 μm) filters. An Amicon multifilter manifold was used in these experiments. The filters, kept under constant vacuum (70 mmHg), were pre-wetted with washing solution (150 mM sucrose, 3 mM $MgSO_4$, and 75 mM of the corresponding salt used in each experiment but with K^+ replacing Rb^+). Within 1 sec, two successive 10-ml applications of ice-cold washing solution were made. The flux time (t) was taken as the time elapsed from the dilution until the initial application of the washing solution. The filters were maintained under vacuum for 1 min and then were placed on tissue paper. After air-drying for 2 hr, the filters were transferred to scintillation vials and the radioactivity was counted on a Packard 4000 Scintillation counter in 10 ml of Hydrofluor (National Diagnostic, NJ). The energy windows of channel *A* and *B* were set between 730 keV and infinity. Channel *A* gain was set at 2%. At this gain, no ^{36}Cl counts could be detected, allowing exclusive measurement of ^{86}Rb. The gain in channel *B* was set at 20%. At this gain, the efficiency for ^{86}Rb was 3.8-fold greater than in channel *A*. Therefore, the ^{36}Cl counts were obtained by subtracting 3.8-fold the channel *A* counts for the total counts in channel *B*. The use of a sixfold larger dosage of ^{36}Cl over ^{86}Rb ensured that the correction for ^{86}Rb counts in channel *B* amounted to less than 20% of the total counts in the channel. The trapped counts at $t = 0$ (C_o) were determined by extrapolation to zero time of the counts for a sample diluted with 3 mM Mn^{2+}. To verify the validity of this determination of C_o, dilutions were also carried in the same solution, but at 0°C, and the extrapolations in both cases were determined. Unless otherwise indicated, the counts at infinite time (C_∞) were determined at t = 70 min. Results are presented as $(C_t - C_\infty)/(C_o - C_\infty)$, where C_t are the counts retained in the filter for the aliquot processed at time t. The trapped volume was calculated as $(C_o - C_\infty)/(C_T \times mg)$, where C_T represents the total counts in the aliquot and mg represents mg protein/ml of the concentrated sample.

H^+ Efflux Studies

Because of the diversity of methods employed, the specific protocols are described in the legends to the figures. The common rationale in all these studies is given in the following. Large H^+ gradients in gastric vesicles are generated via the $(H^+ + K^+)$-ATPase pump by incubation in various ATP-containing media; ATP is then rapidly consumed by a glucose-hexokinase trap, eliminating H^+-uptake activity and allowing the study of H^+-efflux rates (Wolosin & Forte, 1984). Since charge compensation requires that H^+ efflux be matched by concomitant anion co-efflux or cation counterflux, manipulation of the ionic environment allows the use of H^+ efflux rates to monitor cation and anion conductances. H^+ translocation (i.e., ΔpH formation-dissipation) is followed by the changes in fluorescence of the monoamine dye acridine orange. In the absence of a rapidly permeating anion, the ΔpH dissipation represents K^+ influx and is referred to as H^+/K^+ counterflow. In the presence of high intravesicular Cl^-, and at very low external concentration of permeant cation, the ΔpH dissipation represents Cl^--efflux and is referred to as $H^+ - Cl^-$ co-efflux. A third ΔpH dissipation test is based on the ability of anions such as SCN^- to combine with H^+ to form the highly permeable undissociated acid (Gutknecht & Walter, 1981). The rate of H^+ loss reflects then the rate at which the anion can enter the vesicle (Wolosin & Forte, 1984). All H^+ efflux experiments were carried out at 37°C.

Radioisotopes were purchased from New England Nuclear. Methane sulfonate salts were prepared by titration of methane-

sulfonic acid with KOH, RbOH, or N-methylglucamine base (NMG). NMG-Cl was prepared by titration of the base with HCl. Nigericin, valinomycin, and hexokinase (Type 300) were from Sigma. Tetrachlorosalicylanilide (TCS) and acridine orange were from Eastman Kodak. All chemicals used were of highest purity available. Protein was determined according to Bradford (1976) using Cohn fraction II immunoglobulin (Sigma, St. Louis) as standard. K^+-*p*-nitrophenylphosphatase (*p*NPPase) was determined as described by Culp, Wolosin, Soll, and Forte (1983).

Results

Radioisotopic Flux Studies

Although the following experiments were carried out with Rb^+ instead of K^+, we have established in comparative experiments of H^+ uptake the similarity of both cations in the s.a. vesicles.

Kinetic features of the ^{86}Rb and ^{36}Cl efflux from s.a. vesicles under unidirectional and equilibrium exchange conditions are depicted in Fig. 1. Rb^+ exchange was consistently three times faster than Cl^- exchange, even though variations in the actual rates of efflux among various preparations of membranes were noted. The time for half equilibration ($t_{1/2}$) of ^{86}Rb ranged between less than 0.1 min (our time resolution limit) and 0.45 min, and between 0.25 and 1.35 min for ^{36}Cl. The mean and standard deviations for the $t_{1/2}$ values ($n = 8$) were 0.25 ± 0.14 min for ^{86}Rb and 0.78 ± 0.38 for ^{36}Cl. Unidirectional efflux of both Rb^+ and Cl^- proceeded at a pace similar to Cl exchange (Fig. 1*A*). An equivalent result has been reported earlier for influx of KCl and Cl exchange in experiments using $K^{36}Cl$ (Wolosin & Forte, 1983). Replacement of either Cl by methane sulfonate (Fig. 1*B*) or Rb by choline (Fig. 1*C*) reduced the unidirectional efflux of ^{36}Cl or ^{86}Rb, respectively, but there was no pronounced effect on the rates of exchange of the ions. Thus by kinetic criteria, the K^+ and Cl^- pathways could be considered independent of each other (Hopfer & Liedtke, 1981) and in view of the similarity between exchange and unidirectional fluxes, the majority if not all of the exchange fluxes are due to conductive pathways. The main membrane component in s.a. vesicles is the $(H^+ + K^+)$-ATPase. Since the functionally related $(Na^+ + K^+)$-ATPase has been shown to promote a Rb^+ exchange sensitive to vanadate (Beauge, Cavieres, Glynn & Grantham, 1980), and this compound is a potent inhibitor of both ATPases (Faller, Rabon & Sachs, 1983), we tested the effect of vanadate on exchange fluxes. Inclusion of 50 μM vanadate failed to produce any visible change in ^{86}Rb efflux (Fig. 1*C*). At equilibrium, mean and standard deviation for apparent trapped volumes were 1.98 ± 0.56 and 1.53 ± 0.47

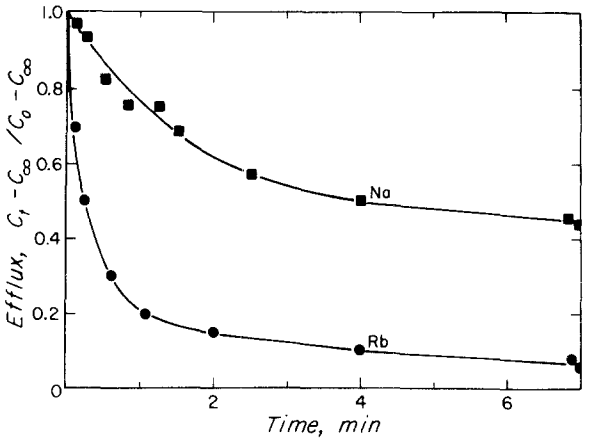

Fig. 2. Comparative exchange of ^{86}Rb and ^{22}Na. Identical batches of membranes were incubated overnight in solutions containing either 75 mM NaCl or 75 mM RbCl. ^{86}Rb or ^{23}Na was added as appropriate and after 2 hr incubation, the samples were diluted in the corresponding unlabeled Rb^+ or Na^+ solutions

when calculated from ^{86}Rb or ^{36}Cl, respectively. The higher trapped volume derived from ^{86}Rb data probably reflects the existence of negative binding sites within the vesicles. These sites will act as cation exchangers, increasing the total concentration of trapped Rb. The specificity of the Rb pathway was tested by comparison of Rb and Na exchange fluxes (Fig. 2). The rate of exchange of Na was approximately 15-fold slower than that of Rb.

In most cases, the time course for isotopic efflux could not be characterized by a single rate constant, suggesting heterogeneity of the vesicular population. It is likely that the observed kinetic heterogeneity arises from the variation in size of the s.a. vesicle population and their complex morphology (Woloson & Forte, 1981*a*). This heterogeneity is exemplified in Fig. 3 which depicts the vesicular size distribution derived from freeze fracture replicas of a typical preparation. Vesicular diameters range from 0.04 to 1.0 μm with an average size of 0.29 μm ($n = 276$). For comparative purposes, the equivalent size distribution of a typical microsomal fraction from resting parietal cells has also been included in Fig. 2. The microsomes range in size between 0.02 and less than 0.2 μm, with an average diameter of 0.098 μm ($n = 90$). It should be noted that in spite of the difference in size distribution, the $(H^+ + K^+)$-ATPase activity of both vesicular preparations are similar. The reasons for the difference in size and morphology between both $(H^+ + K^+)$-ATPase-rich vesicular types are beyond the scope of this article. It has been suggested that the differences result from the membrane fusion process and interactions of $(H^+ + K^+)$-ATPase membrane with microfilaments during stimulation of the oxyntic

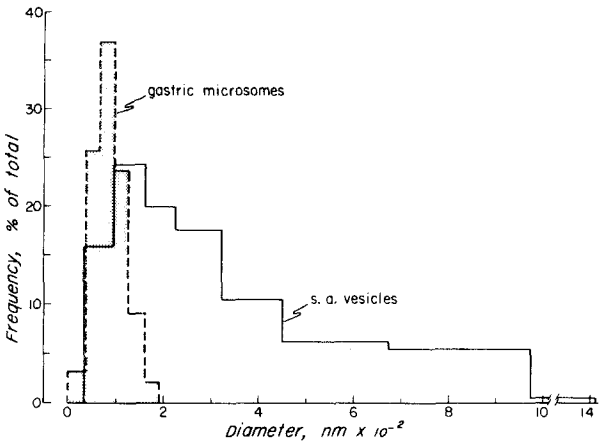

Fig. 3. Histogram for vesicular size distribution of $(H^+ + K^-)$-ATPase-rich vesicles. The outer diameters were measured from micrographs of freeze-fracture replicas of gastric microsomes and s.a. vesicles. The figure depicts the percent of vesicles within certain size limits. Total vesicles measured was 90 for gastric microsomes and 276 for s.a. vesicles

Table. The effect of divalent cations on the relative rates of ^{86}Rb and ^{36}Cl effluxes under equilibrium exchange conditions

M^{2+} cation	$t_{1/2}/t^c_{1/2}$	
	Rb	Cl
Mg (1 mM)	1.0	1.0
Ca (0.5 mM)	1.0	1.1
Ba (0.5 mM)	2.0	1.0
(1.0 mM)	2.4	0.9
(3.0 mM)	3.6	1.0
Mn (0.5 mM)	2.8	2.8
Co (0.5 mM)	2.6	2.4
Ni (0.5 mM)	3.0	2.6
Zn (0.1 mM)	3.9	3.4

Aliquots of concentrated vesicle suspension pre-equilibrated with double labeled RbCl solution as described in Materials and Methods were incubated for 30 sec with the indicated concentrations of cations and diluted with 19 volumes of unlabeled RbCl solution complemented with the same divalent cation. The time course of isotopic efflux was followed by aliquot filtration. Experimental times for half equilibration ($t_{1/2}$) were derived from plots of trapped radioactivity as a function of time and are presented as the ratio between the $t_{1/2}$ with divalent cations and the control ($t^c_{1/2}$) without them.

cell (Wolosin & Forte, 1981*a*). Because of the relationship between the apparent rate constant for equilibration and the volume to area ratios, the wide range in s.a. vesicles is likely to generate a heterogeneity in the kinetics of isotopic fluxes. The observation that the kinetic patterns were preserved following inhibition with Mn^{2+} and reactivation with

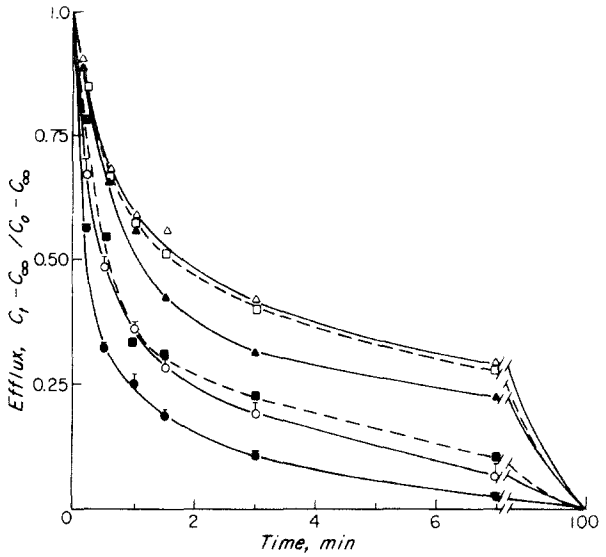

Fig. 4. Effect of Mn^{2+} on the efflux of ^{86}Rb and ^{36}Cl under equilibrium exchange conditions. Experimental procedure was as described in Materials and Methods and Fig. 1*A*. Control conditions are shown for ^{86}Rb (●) and ^{36}Cl (○) efflux. The vertical bars represent the variance between efflux experiments with the same pre-equilibrated vesicular preparation. Addition of 2 mM Mn^{2+} greatly slows the efflux of both Rb (▲) and Cl (△). Also shown are the results in the presence of 2 mM Mn^{2+} and 2.5 μM nigericin for Rb (■) and Cl (□). All lines are drawn by eye

nigericin (e.g., *see* Fig. 4) is also consistent with the hypothesis of physical (size), rather than chemical, heterogeneity.

Divalent cations affected Rb^+ and Cl^- fluxes. Figure 4 depicts the changes in efflux rates under equilibrium exchange conditions when Mn^{2+} or Mn^{2+} plus nigericin were included in the dilution medium. Both exchange rates were inhibited by Mn^{2+}. Introduction of nigericin restored Mn^{2+}-inhibited Rb^+ fluxes towards control values while the Cl^- fluxes remained unchanged.

Studies were also carried out with other divalent cations. Comparative results are summarized in the Table. The rapidity of the exchange, particularly in the case of Rb, precluded the use of initial rates as a viable kinetic parameter; therefore, the relative time for half equilibration ($t_{1/2}$ experimental/$t_{1/2}$ control) was used for quantification. Mg^{2+} and Ca^{2+} did not significantly alter the control rates of exchange for either Cl or Rb. Ba^{2+}, at mM concentrations, inhibited exclusively the Rb^+ exchange without affecting the Cl^- fluxes. Zn^{2+}, Mn^{2+}, Co^{2+}, and Ni^{2+} inhibited both fluxes. Zn^{2+} was the more powerful inhibitor, while the three transition metals were roughly equipotent.

Since both anion and cation fluxes were inhibited by several divalent cations, concentration de-

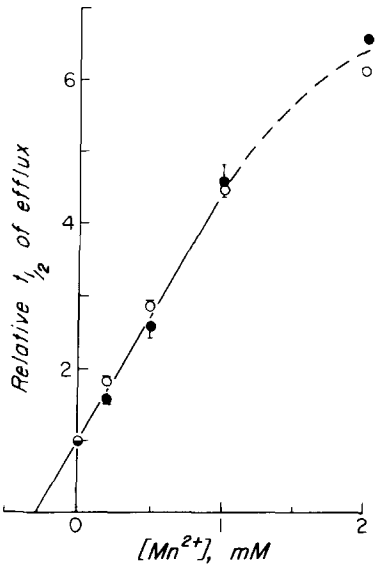

Fig. 5. The rate of exchange of ^{86}Rb and ^{36}Cl as a function of the concentration of Mn^{2+}. The indicated Mn^{2+} concentration was added to aliquots of the concentrated vesicle suspensions that had been pre-equilibrated with double labeled RbCl. Fifteen seconds later the exchange efflux was started by diluting in unlabeled incubation medium complemented with the indicated concentration of Mn^{2+}. Relative rate of efflux was taken as the experimental $t_{1/2}$ divided by the $t_{1/2}$ in the absence of Mn^{2+} for both ^{86}Rb (●) and ^{36}Cl (○). The vertical lines represent variance for two experiments with different membrane preparations

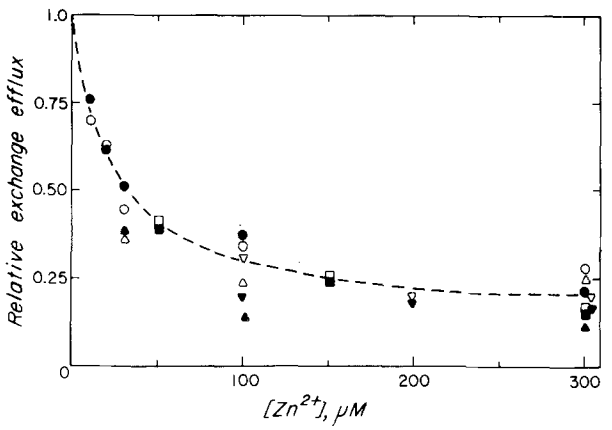

Fig. 6. The effect of Zn^{2+} on the relative rate of exchange. The relative exchange efflux was calculated as the $t_{1/2}$ of control divided by $t_{1/2}$ in the presence of Zn^{2+}. Experimental details are as in Fig. 5, but 1 mM Mg^{2+} was included along with the various concentrations of Zn^{2+}. The relative exchange fluxes for Rb^+ are given by full symbols and for Cl^- by open symbols. The different symbols represent various vesicular preparations

pendence studies were carried out in order to assess the concurrence of both effects. Figure 5 depicts the effect of Mn^{2+} on the relative $t_{1/2}$ values for Rb and Cl. Because $t_{1/2}$ is proportional to $1/k$, where k is the rate constant of exchange, the plot is analogous to a $1/v$ vs. inhibitor (I) concentration, i.e., a Dixon plot. It is clear that the action of Mn^{2+} on both permeabilities in the 0 to 1 mM range complies with the equation $t_{1/2} = t^0_{1/2}/(1 + [Mn^{2+}]/K_I)$, where $t^0_{1/2}$ is the half-time for equilibration in the absence of divalent cation and K_I is the constant of inhibition equal to 250 μM. Above 1 mM Mn^{2+}, the extent of inhibition tended to saturate, i.e., Mn^{2+}-insensitive components of Cl and Rb exchange existed. In the presence of 3 mM Mn^{2+}, the isotopic exchange rate ranged from 8–17% of the control rates in various experiments.

Figure 6 depicts, in a different format, the concurrent inhibitory effect of Zn^{2+} on Rb^+ and Cl^- exchange fluxes. A K_I between 20 and 30 μM for the main component of the ion flux can be inferred. These experiments with low Zn^{2+} were carried out in the presence of 1 mM Mg^{2+}. Exclusion of Mg^{2+} from the assay medium resulted in an apparent increase in the K_I for Zn^{2+}. A likely reason for this potentiating effect of Mg^{2+} on Zn^{2+}-inhibition may be found in the characteristics of divalent ion binding to nonspecific membrane sites. When Zn^{2+} is the only divalent ion, the actual free concentration of Zn^{2+} decreases. The nonspecific binding is likely to be reduced when Mg^{2+} is included as a screening agent. Thus, an accurate determination of K_I for Zn^{2+} will require the development of a Zn^{2+} buffering system to insure levels of free cation, insensitive to changes in the concentration of membrane binding sites or competing divalent cations.

Concentrations of Zn^{2+} above 0.3 mM had, under certain experimental conditions, a complex effect on the exchange fluxes. (These experiments were prompted by observation of the effect of Zn^{2+} on H^+/K^+ counterflux to be described in the following section.) When concentrated vesicle suspensions, preloaded with ^{86}Rb and ^{36}Cl, were pre-incubated for several minutes in, or above, 0.4 mM Zn^{2+} prior to dilution with the isotope-free solution, high inhibition of Cl exchange flux was observed. Rubidium exchange was only partially affected. We also noted, both by visual observation and by following the turbidity of membrane suspensions in the spectrophotometer, that at and above 0.4 mM, Zn^{2+} induced a vesicle aggregation which was not readily reversible. There was no measurable effect on trapped volume of the preparations. The aggregation phenomena was not observed with the other cations in the concentration ranges studied here. It is possible that strong binding of Zn^{2+} to membrane sites induces a re-organization as a result of which the previous action of low Zn^{2+} concentrations is modified and the inhibition of the Rb pathway is relieved while the inhibition of the Cl pathway remains unchanged or increases.

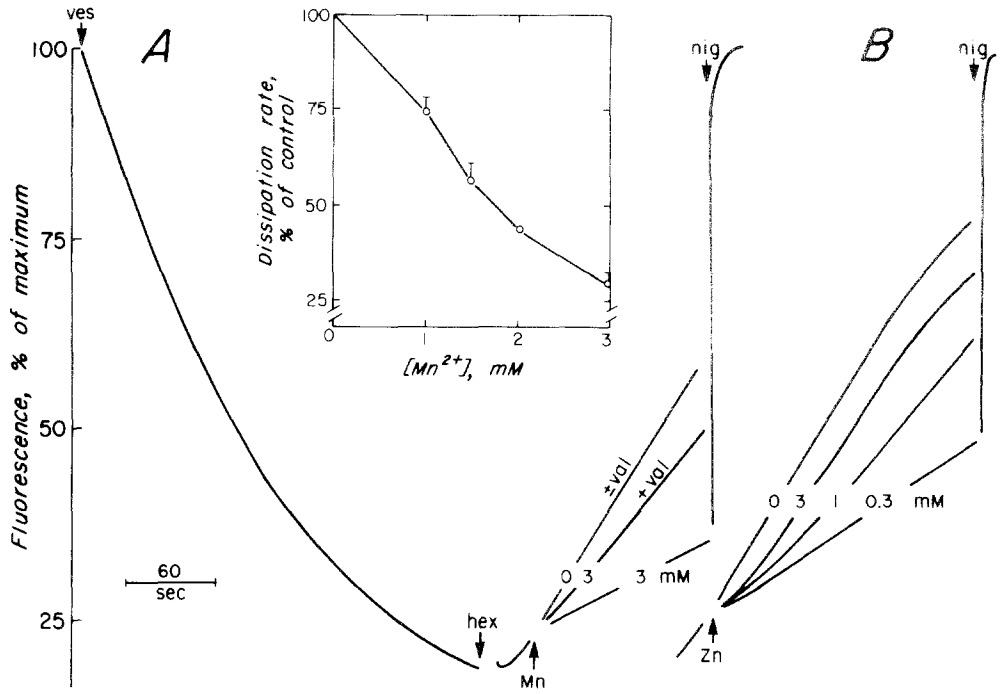

Fig. 7. Effect of Mn^{2+} and Zn^{2+} on H^+ efflux under conditions of H^+/K^+ counterflux. Stimulation-associated vesicles (60 μg) were added to H^+ uptake medium consisting of 1.2 ml of 100 mM K methane sulfonate, 100 mM sucrose, 10 mM glucose, 4 mM Tris-TES, 2 μM acridine orange, 1 mM $MgSO_4$, and ATP (0.4 mM ATP in the Mn^{2+} experiments or 0.1 mM ATP in the Zn^{2+} experiments). The development of H^+ gradient was followed by the quenching of acridine orange fluorescence. After significant gradients developed, H^+ pumping was arrested by addition of 30 μg hexokinase (*hex*) to consume all ATP, and the rate of ΔpH dissipation was followed. (*A*): Effects of Mn^{2+} and valinomycin. The control rate of H^+ efflux that occurs in exchange for incoming K^+ is not modified by the inclusion of valinomycin (± *val*). Addition of Mn^{2+} slows the rate of ΔpH dissipation. The inhibition is much smaller when the K^+ ionophore valinomycin is present. *Inset:* The dependence of the rate of H^+ efflux on the concentration of Mn^{2+}. The results represent the change in rate of fluorescence recovery when the control rate (slope) is taken as 100%. (*B*): Effects of Zn^{2+}. Addition of Zn^{2+} at 0.3 mM produced a reduction in the rate of H^+ efflux similar to that seen with 3 mM Mn^{2+}. Higher concentrations of Zn^{2+}, however, restored rates of H^+ efflux toward control. Full gradient dissipation was rapidly elicited in all cases by addition of 10 μM nigericin (*nig*)

ΔpH Dissipation by $H^+ - K^+$ Counterflow

Figure 7*A* depicts the pattern of ΔpH formation in K-methane sulfonate as well as patterns for dissipation following the consumption of ATP by hexokinase. It can be seen that: (i) the H^+ uptake and dissipation rates were not altered by valinomycin; (ii) addition Mn^{2+} had an inhibitory effect on the dissipation rate; (iii) valinomycin reversed the inhibition, demonstrating that the effects of Mn^{2+} are at least in part due to inhibition of K^+ permeability; (iv) in contrast to Mn^{2+}, neither Mg^{2+} nor Ca^{2+} altered the dissipation rate. Co^{2+} and Ni^{2+} produced an inhibition very similar to Mn^{2+}. A quantitative comparison has not been made because these two cations tended to quench the fluorescent signal (e.g., 20% quenching for 3 mM Co^{2+}). The dependence of the rate of dissipation on the total concentration of free Mn^{2+} is presented in the inset. The dissipation rate decreased with the increase in Mn^{2+} concentration. More than 1 mM Mn^{2+} was necessary to achieve a 50% decrease in dissipation rate.

A similar study was carried out for Zn^{2+} (Fig. 7*B*). At 300 μM, this cation produced a slightly stronger inhibition of ΔpH dissipation than 3 mM Mn^{2+}. But when the concentration of Zn^{2+} was raised, the inhibitory effect was gradually eliminated. Since we had observed precipitation by Zn^{2+} with the more concentrated solutions used in radioisotopic studies, we monitored the turbidity of the suspensions under the conditions of the experiment. No turbidity changes were detected in this case, due probably to the very low amount of protein used and/or the higher temperature.

ΔpH Dissipation by $H^+ - Cl^-$ Co-Efflux

Figure 8 depicts the dissipation patterns observed from vesicles in which the ATP-generated pH gradient was first formed in 30 mM KCl and then diluted 21-fold with KCl-free solutions. In the absence of divalent cations, the leak of HCl proceeded rapidly. We have previously demonstrated that this leak is

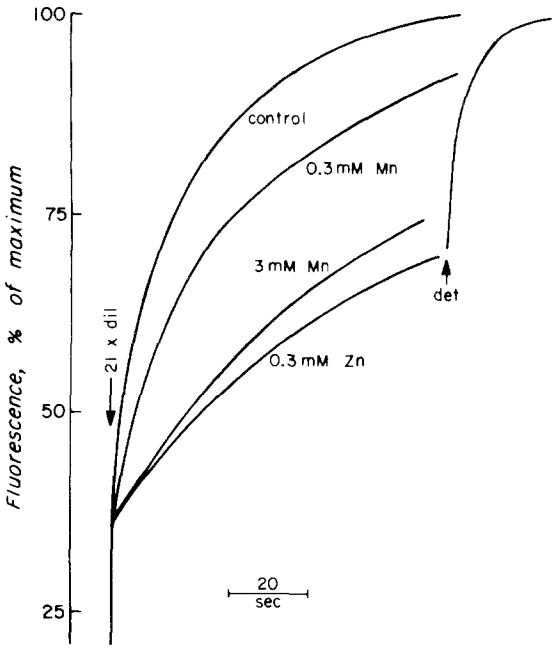

Fig. 8. Effect of Mn^{2+} and Zn^{2+} on H^+ efflux under conditions of $H^+ - Cl^-$ co-efflux. Stimulation-associated vesicles (60 μg) were incubated in a total volume of 0.06 ml containing 30 mM KCl, 250 mM sucrose, 10 mM glucose, 50 mM Tris-TES, 4 mM MgATP, 0.2 mM EDTA, pH 7.25. After 3 min, 30 μg (2 μl) hexokinase was added. Twenty seconds later the samples were diluted with 1.2 ml of 330 mM sucrose complemented with divalent cations as indicated (arrow at 21 × *dil*). Full and rapid fluorescence recovery was elicited in all cases by addition of 0.02% Triton X-100 (*det*)

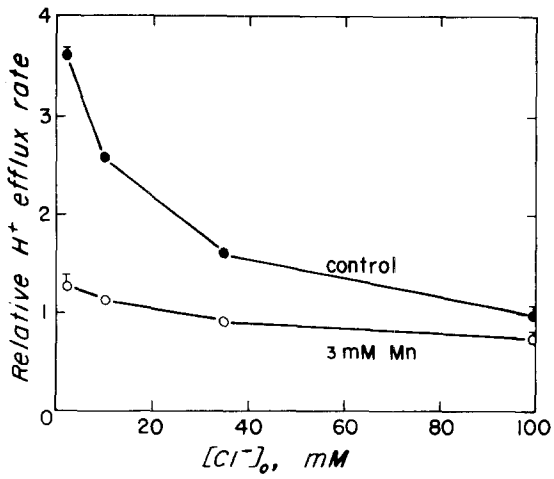

Fig. 9. Inhibition of $H^+ - Cl^-$ co-efflux by Mn^{2+} as a function of extravesicular Cl. Concentrated s.a. vesicles were incubated as described in Fig. 8 to produce an ATP-generated ΔpH and after 3 min, ATP was eliminated by adding hexokinase. Twenty seconds later, the samples were diluted with 1.2 ml of a solution composed of 100 mM sucrose and mixtures of 100 mM N-methylglucamine methanesulfonate and 100 mM N-methylglucamine Cl to attain the specified Cl concentrations. Efflux rates were determined from the rate (slope) of fluorescence recovery at the same level of fluorescence (40% of maximum) and are plotted as relative to the rate in the presence of 100 mM Cl^- without Mn^{2+}, which is taken arbitrarily as 1.0. Results are shown for control (●) and when 3 mM Mn^{2+} (○) was included in the diluting solution

primarily due to the Cl-gradient driven H^+ efflux through independent ionic pathways (Wolosin & Forte, 1984). Introduction of certain divalent cations had pronounced effects on the rates of ΔpH dissipation. For Zn^{2+}, 300 μM produced a large reduction in H^+ efflux. As the concentration of Zn^{2+} was raised, no further inhibition of the dissipation was observed. For Mn^{2+}, the inhibition increased as the cation concentration was raised. Ni^{2+}, at 2 mM, had an effect similar to Mn^{2+}. Neither Ca^{2+} nor Mg^{2+} (3 mM each) altered the dissipation rates from control.

If the concentration of Cl^- in the K^+-free diluting solution is raised, the rate of ΔpH dissipation decreases in a manner that can be simulated by assuming that the efflux of H^+ is a function of the membrane potential (ψ_m) and that the latter depends only on the transmembrane $[Cl^-]$ gradient, i.e., $P_{Cl}[Cl^-]_i > P_H[H^+]_o$ and $P_{Cl}[Cl^-]_o > P_H[H^+]_i$ even when $[Cl^-]_o$ is very small (Wolosin & Forte, 1984). For this report, the inhibition of HCl efflux by 3 mM Mn^{2+} at various concentrations of external Cl was studied. The results are depicted in Fig. 9. Manganese has a very small effect on the rate of H^+ dissipation for $[Cl^-]_o$ = 100 mM. As the concentration of Cl was decreased, and the rate of dissipation of the control increased, the inhibitory effect of Mn^{2+} became more pronounced and the dependence on $[Cl^-]_o$ was almost eliminated. These results are consistent with the notion that the inhibition of dissipation by Mn^{2+} is due to a change in P_{Cl} and not P_H so that at the low Cl range, the criterion that $P_{Cl}[Cl^-]_o > P_H[H^+]_i$ no longer holds. Similar attenuation of the dependence of $[Cl^-]_o$ was attained in our previous work (Wolosin & Forte, 1984) by increasing P_H with a H^+ ionophore.

NO_2^- and SCN^--induced ΔpH Dissipation

SCN^- and NO_2^- inhibit acid secretion in whole gastric mucosa. Studies in black lipid membranes (Gutknecht & Walter, 1981) and isolated gastric vesicles (Reenstra & Forte, 1982; Wolosin & Forte, 1983) have demonstrated that the action of SCN^- is due to its capacity to penetrate through the s.a. membrane and combine with H^+ forming the highly permeable acid, which is then able to leave the vesicle as a highly membrane-permeable species. Thus the increase in pH dissipation induced by SCN^- reflects its rate of vesicular penetration, i.e., J°_{HSCN}

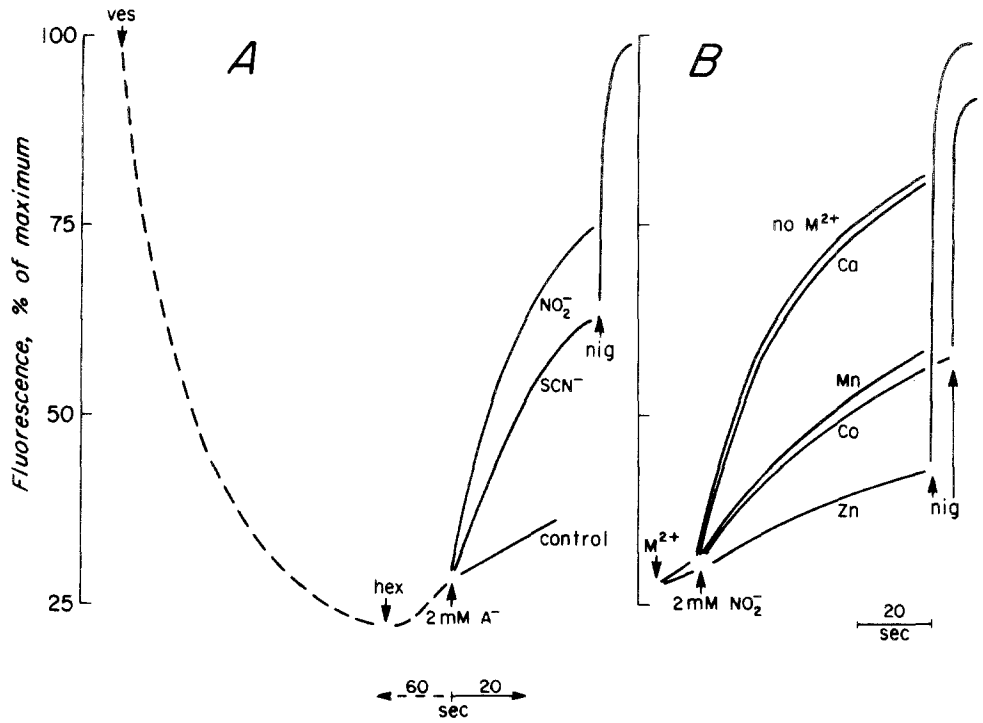

Fig. 10. Increase in ΔpH dissipation by NO_2^- and SCN^-, and effects of divalent cations. Stimulation-associated vesicles (60 μg) were added to 1.2 ml containing 50 mM K_2SO_4, 10 mM Cl, 150 mM sucrose, 10 mM glucose, 4 mM, Tris-TES, 0.4 mM $MgSO_4$, 0.4 mM ATP, 2 μM acridine orange, pH 7.25. The development and dissipation of H^+ gradients were followed by the quenching of acridine orange fluorescence. H^+ uptake was arrested by consumption of ATP with 30 μg hexokinase (*hex*). (*A*): H^+ gradient formation and the effect of NO_2^- and SCN^- on the ΔpH dissipation. Note the change in chart speed used to measure ΔpH dissipation rates. ΔpH dissipation was increased by addition of 2 mM $NaNO_2$ or NaSCN. (*B*): Effects of divalent cations on NO_2^--induced ΔpH dissipation rates. Prior to addition of 2 mM NO_2^-, 1 mM of various divalent cations were added (M^{2+}). In all cases, full fluorescence recovery could rapidly be elicited with 10 μM nigericin (*nig*). However, Co^{2+} caused quenching of the fluorescence of free acridine orange

$= J^i_{SCN}$, where J^e_{HSCN} represents the SCN^--induced proton efflux and J^i_{SCN} the net influx of SCN^-. This latter influx could be compensated by entry of extravesicular K^+ or exit of intravesicular anion. In the past, we conducted studies only with SCN^- in the presence of H^+ pumping (Wolosin & Forte, 1983). For the present report, control studies were conducted to determine the similarity of action of SCN^- and NO_2^- after H^+ pumping activity was arrested. The H^+ uptake media selected for these experiments, K_2SO_4-KCl favors SCN^- or NO_2^- entry by providing an outwardly direct Cl^- gradient and an inwardly directed K^+ gradient after the formation of the ΔpH. Figure 10 shows that both anions had similar effects on the rate of ΔpH dissipation. For large H^+ gradients NO_2^- was twice as powerful as SCN^-; SCN^- became even less effective as the ΔpH decreased. This is an expected result: SCN^- is a much stronger acid than NO_2^- and therefore is less effective in transporting H^+ as the internal pH approaches neutrality. For NO_2^-, the rate of dissipation increased linearly up to about 8 mM, suggesting that in this concentration range, the introduction of the anion did not modify the driving forces (membrane potential, ionic gradients) acting on its rate of transport.

The effect of divalent cations on the NO_2^- induced dissipation rate is shown in Fig. 10*B*. Zn^{2+}, Mn^{2+}, Ni^{2+}, and Co^{2+} inhibit the NO_2^--induced dissipation of ΔpH while Mg^{2+} and Ca^{2+} have no effect. For Mn^{2+} and Zn^{2+}, a concentration dependence was performed. In these experiments, ATP was reduced to 0.2 mM to decrease sequestration of the divalent cations. The results are presented in Fig. 11 where the free concentrations of divalent cations were calculated taking into account cation complexation by SO_4^{2-}. The concentration for 50% inhibition (I_{50}) of the NO_2^--induced dissipation occurred at approximately 10 μM for Zn^{2+}, and 100 μM for Mn^{2+}. Studies performed with SCN^- yielded similar results. However, a fraction of the SCN^--induced ΔpH dissipation increase was resistant to inhibition, a result which can possibly be attributed to the existence of a significant, lipophilic pathway for penetration of this hydrophobic anion (Berry & Hinkle, 1983).

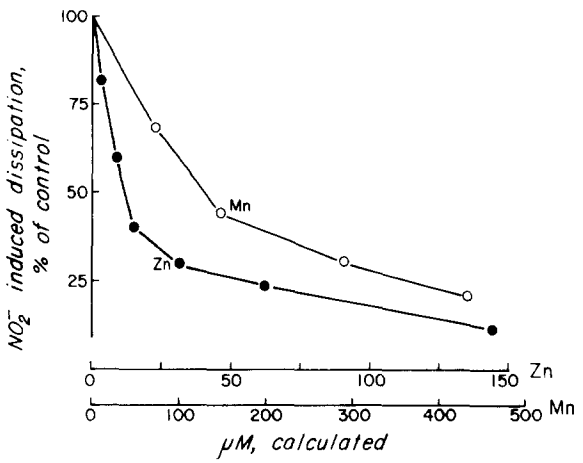

Fig. 11. The dependence of NO_2^--induced ΔpH dissipation on the concentration of divalent cations. H^+ uptake proceeded in K_2SO_4-KCl medium as described for Fig. 10, but the concentration of ATP was decreased to 0.2 mM. After consumption of ATP by hexokinase, Mn^{2+} or Zn^{2+}, followed by 2 mM $NaNO_3$, were added. The NO_2^--induced dissipation represents the difference between the rate of fluorescence recovery before and after addition of NO_2^-. Results are presented as percent of the difference from the control. The free concentrations of Zn^{2+} and Mn^{2+} (calc M^{2+}) were calculated from the total concentration of Mn^{2+} and Zn^{2+}, the concentration of free SO_4^{2-}, and stability constants for $MnSO_4$ and $ZnSO_4$ equal to 200 (Dawson, Elliot, Elliot & Jones, 1969). Free concentration of SO_4^{2-} was calculated from the total concentration of K^+ and SO_4^{2-}, and a stability constant for KSO_4 equal to 9.4 derived from colligative properties of K_2SO_4 solution

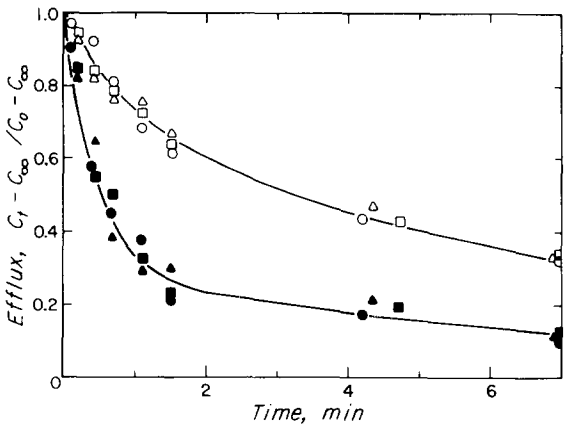

Fig. 12. ^{86}Rb and ^{36}Cl efflux from gastric microsomes under equilibrium exchange conditions. Gastric microsomes (8 mg/ml) in 300 mM were mixed with an equal volume of 150 mM RbCl, 8 mM Tris-TES, pH 7.25, containing both ^{86}Rb and ^{36}Cl. To follow the uptake of isotopes, small aliquots were filtered at appropriate intervals. The $t_{1/2}$ of RbCl equilibration exceeded 10 min and complete equilibration required 4 hr at 23°C. After equilibration was established, 1 mM $MgSO_4$ was added and the incubation batch was split into three fractions. One fraction was complemented with vanadate (100 μM) and another with Zn^{2+} (200 μM). Two minutes later, isotopic efflux was initiated by the addition of 19 volumes of 150 mM sucrose, 75 mM RbCl, 4 mM Tris-TES, 1 mM $MgSO_4$, and, where appropriate, complemented with 100 μM vanadate or 200 μM Zn^{2+}. ^{86}Rb efflux is shown for control (●), Zn^{2+} (▲), and vanadate (■); ^{36}Cl efflux is shown for control (○), Zn^{2+} (△), and vanadate (□). K^+-stimulated *p*NPPase activity was measured separately by adding the microsomes to the diluting solutions complemented with 5 mM *p*NPP. With Zn^{2+} the *p*NPPase activity amounted to 28% of control; with vanadate, *p*NPPase activity was not detectable

Test for Nonspecific Changes in Membrane Properties

Binding of divalent cations to membrane surfaces could affect transport phenomena by mechanisms other than specific inhibition. Inhibition may result from changes in surface charge (Bernardt, Donath & Glaser, 1984) or in the fluidity of the membrane core (Housley & Stanley, 1982). Two tests yielding information about membrane fluidity were performed. The effect of 3 mM Mn^{2+} on ΔpH dissipation by nigericin under the conditions of $H^+ - K^+$ counterflow was investigated using two concentrations of the K^+/H^+ exchange ionophore, 0.5 and 5 μM. For a small carrier molecule, to the extent that carrier diffusion depends on viscosity, a change in membrane fluidity will change transport capacity as demonstrated by Stark, Benz, Pohl and Janko (1972). The nigericin-induced rates of ΔpH dissipation were not affected by Mn^{2+}. A second test was made using 12 doxyl stearic acid as an electron paramagnetic probe for changes in membrane fluidity (Tourtellotte, Branton & Keith, 1970). The EPR spectra from control membrane samples in the RbCl solution were compared against experimental samples complemented with 2 mM of either Ca^{2+}, Co^{2+}, Ni^{2+} or Zn^{2+}. The width of signal from the membrane-dissolved probe was not modified by any of the divalent cations, suggesting that the cations have no effect on membrane fluidity. Changes in surface charge are an unlikely source of inhibition for transport of both positive and negative ions.

Comparative Studies on Gastric Microsomal Vesicles

The classical microsomes associated with nonsecreting tissue have low K^+ and Cl^- permeabilities and thus are unable to accumulate acid efficiently (Rabon, Takeguchi & Sachs, 1980; Wolosin & Forte, 1984). It is not known if the permeabilities present reflect nonspecific leak pathways or a low activity of the pathways expressed in the s.a. vesicles. Therefore, the effect of divalent cations on these pathways was studied as a means to discriminate between the two possibilities. Both radioisotopes and the ΔpH dissipation approach were used.

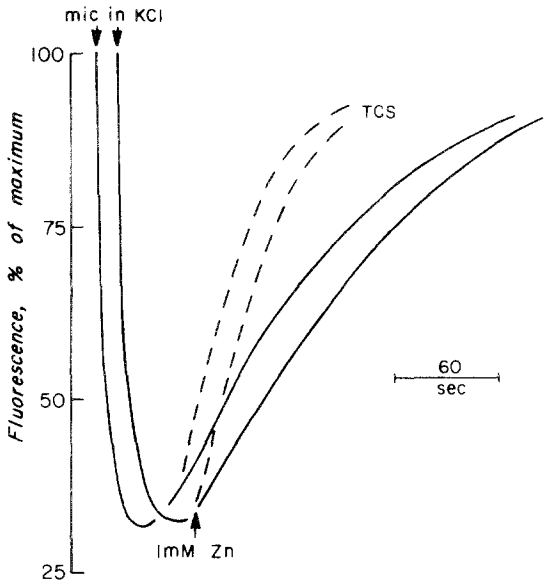

Fig. 13. Effect of Zn^{2+} on $H^+ - Cl^-$ co-efflux in microsomes. 20 μl (120 μg) of microsomes were pre-incubated for 2 hr in 200 mM KCl, and then added to 1.2 ml of 400 mM sucrose, 4 mM Tris-TES, 0.4 mM $MgSO_4$, 0.4 mM NaATP, 2 μM acridine orange. Rapid fluorescence quenching results from ATP-driven H^+/K^+ exchange. When intravesicular K^+ is depleted, the gradient dissipates. Dissipation is increased by addition of 2 μM of the H^+ ionophore tetrachlorosalicylanilide (*TCS*) shown by dashed lines. Addition of 1 mM Zn^{2+} does not modify either the spontaneous or TCS-induced $H^+ - Cl^-$ co-efflux

Figure 12 depicts the time course of ^{36}Cl and ^{86}Rb isotopic efflux in gastric microsomes under equilibrium exchange conditions. Though not shown, the ^{86}Rb and ^{36}Cl influx rates were also measured. The following observations were made: (i) as reported in the past, the influx of Rb and Cl is slow, with a $t_{1/2}$ of between 10 and 20 min; (ii) in spite of its slow unidirectional influx, ^{86}Rb efflux under equilibrium exchange was fast ($t_{1/2} \approx 0.5$ min); (iii) ^{36}Cl efflux under equilibrium exchange conditions was much slower than ^{86}Rb, but still significantly faster than the Cl influx; (iv) both Rb^+ and Cl^- fluxes in either unidirectional or exchange conditions were not affected by Zn^{2+} or VO_4^{3-}; (v) both Zn^{2+} and vanadate inhibited enzymatic activity.

The effect of Zn^{2+} on unidirectional Cl^- efflux was also studied under H^+ and Cl^- co-efflux conditions (Fig. 13). An HCl gradient was induced by suspending KCl equilibrated microsomes in sucrose complemented with MgATP. Following utilization of all available trapped K^+ by the pump, the formed ΔpH gradually dissipated by the co-efflux of H^+ and Cl^-. Unlike the case of s.a. vesicles, the divalent cations did not inhibit the ΔpH dissipation in the microsomal vesicles.

Discussion

Rb and Cl Pathways in S.A. Vesicles

The rates of Rb^+ and Cl^- fluxes in s.a. vesicles were studied radioisotopically. Under equilibrium exchange conditions, the Rb flux is threefold faster than Cl. Replacement of Rb or Cl by impermeant ions does not modify the rates of ion exchange, indicating the independence of cation and anion pathways. Efflux of RbCl proceeded at a rate similar to the rate of Cl equilibrium exchange. In view of the lack of interaction between anion and cation transport, the similarity between unidirectional and exchange fluxes implies that the Rb^+ and Cl^- pathways are either completely, or at least predominantly, conductive.

The use of divalent cations provided an interesting insight into the relationships between these stimulation-associated pathways. Ba^{2+}, as typical for this cation, inhibited the Rb exchange without effect on Cl fluxes, consistent with the functional independence of both ion pathways. The Ba^{2+} effect on other K^+ channels has been attributed to a competitive interaction with the K^+ binding site due to the similarity in the ionic radius of both cations (Latorre & Miller, 1983). Mn^{2+} and other transition metals, as well as Zn^{2+}, were found to have a concurrent inhibitory effect on both Rb^+ and anion transport. This was a surprising finding in view of the functional independence of these pathways.

The effect of divalent cations on ΔpH dissipation was also studied. The main purpose of such experiments was to establish the extent of correlation between the permeabilities studied radioisotopically and the conductive pathways observed in the s.a. vesicles derived from the oxyntic cell apical membrane. Ionic conditions were widely different in both cases (temperature, H^+ gradients, ionic gradients). Nevertheless, a nonequivocal correlation was established: Zn^{2+}, Mn^{2+}, Co^{2+}, and Ni^{2+} inhibited all dissipation processes that were dependent on either K^+ influx or Cl^- efflux, and the relative inhibitory potency of Zn^{2+} and Mn^{2+} was the same as that found in the experiments with radioisotopes. In addition, reversal of inhibition of Rb flux by high Zn^{2+} concentrations was also observed. Recovery of ΔpH dissipation by valinomycin in $H^+ - K^+$ counterflow, and the modification by Mn^{2+} of the dependence of H^+ efflux on extravesicular Cl^- in $H^+ - Cl^-$ co-efflux, demonstrate that the inhibitory effect of the divalent cations is primarily due to their effect on K^+ and Cl^- permeabilities rather than to inhibition of H^+ permeability. Small effects of the divalent cations on H^+ permeability, though, could not be completely ruled out. The percent inhibition of ΔpH dissipation under conditions of $H^+ - K^+$

counterflow and $H^+ - Cl$ co-efflux for a given Mn^{2+} concentration was much smaller than the percent inhibition of Rb^+ and Cl^- isotopic flux. The contradiction between these results is only apparent. Given the nature of the Goldman-Hodgkin-Katz relationships for membrane potentials and ionic fluxes (J), a 10-fold decrease in permeability (P_K or P_{Cl}) is not expected to result in an equivalent decrease in H^+ efflux. In fact, unless all ion concentrations and permeabilities are known, it is impossible to predict the extent of change in H^+ efflux.

Divalent cations also inhibited NO_2^- and SCN^- flux, demonstrating that transport of these frequently used inhibitors of gastric secretion occurs by the same pathway as Cl^-. The inhibition of NO_2^--induced dissipation was characterized by K_I values somewhat lower than the values observed in the isotopic flux experiments. Conceivably, the divalent cations could inhibit NO_2^- influx, not only through their effect on anion permeability to which the anion influx is linearly related, but by decreasing P_K, P_{Cl} and thus decreasing the driving force for NO_2^- influx. In any event, the similarity of K_I values for isotopic exchange fluxes and NO_2^--induced dissipation suggest that intravesicular acidification has no significant effect on binding of divalent cations.

The concurrence of anion and cation transport inhibition by divalent cations invites two alternative explanations. It is possible that the Rb and Cl pathways are physically separated. In such a case, the reversal of inhibition by high $[Zn^{2+}]$ could be explained by any mechanism localized to the Rb pathway. However, such a hypothesis requires the coincidental concurrence of inhibition of both pathways by four different divalent cations. In this context, it could be speculated that the concurrent inhibition of K(Rb) and Cl fluxes is due to effects on membrane properties rather than to specific binding to inhibitory sites on the transport entities. Our attempts failed to produce any indication favoring these possibilities. Thus, binding to specific site(s) is the more likely reason for the observed inhibition. We would suggest then that in spite of their functional independence, the Rb and Cl pathways are housed within a single domain or protein. Binding of divalent cation to an allosteric site might affect the conformation of this protein in a way that turns off transport (e.g., in the case of fluctuating channels, the binding of divalent cation might alter the open-close fluctuation, displacing them toward the closed position).

Rb and Cl Pathways in Microsomes

The findings reported here for rabbit microsomes are consistent with those reported earlier for microsomes from hog (Schackmann, Schwartz, Saccomani & Sachs, 1977). While RbCl influx is a slow process, Rb exchange is very fast. From the $t_{1/2}$ of 10–20 min for Rb influx and 0.5 min for exchange, a 20- to 40-fold difference is revealed. Since Cl exchange also proceeds faster than RbCl influx, it is evident that at least one of the exchange processes represents obligatory exchange. We have shown recently that K^+ conductive permeability in the microsomes is extremely low and, in fact, almost indistinguishable from Li^+ conductance (Wolosin & Forte, 198); thus, the Rb^+ exchange must represent an electroneutral process.

In stark contrast to the results in s.a. vesicles, the exchange and unidirectional ion fluxes as well as H^+ and Cl co-efflux in gastric microsomes were completely unaffected by Zn^{2+}; thus, we could conclude that no vestiges of the divalent ion-sensitive permeabilities found in the stimulation-associated membranes are detectable in the microsomes. On the other hand, comparison of the $t_{1/2}$ for Rb exchange in both vesicular types brings up the following question: Is the fast Zn^{2+}-insensitive Rb^+ exchange of gastric microsomes absent or reduced in the s.a. vesicles? In order to address this question, it must be recalled that equilibration times are directly proportional to the volume/area vesicular ratio, i.e., to vesicular radius. Since s.a. vesicles are several-fold larger than the microsomes, the $t_{1/2}$'s for the Zn^{2+}-insensitive Rb and Cl exchange will be proportionally longer. Thus, in the s.a. vesicles, these processes could contribute to the observed Zn^{2+} and Mn^{2+}-insensitive components, which are a fraction of the sensitive component.

Implications for the Physiology of the Oxyntic Cell

The use of divalent cations as inhibitors of transport suggests a physical link between functionally independent K^+ and Cl^- permeabilities expressed by the s.a. vesicles and establishes that these permeability pathways are completely absent in the microsomes. Within the framework of the morphological changes in the oxyntic cell and the fusion recycling model (Forte et al., 1977), two mechanisms, at least, can be conceived to explain the appearance of the ionic conductances in the $(H^+ + K^+)$-ATPase membrane. It is possible to position the conductive pathways in the permanent apical membrane of the nonsecreting cell which has been shown to be distinct from the tubulovesicular membrane (Black, Forte & Forte, 1981; Smolka, Helander & Sachs, 1983), implying then that confluence with the $(H^+ + K^+)$-ATPase membrane is the result of fusion of the tubulovesicles with that membrane. In their simplest interpre-

tation, our results with the divalent cations favor that possibility. In the nonsecretory state, in order to avoid loss of KCl from the cell, the KCl pathways will have to be repressed. Alternatively, the ionic pathways could be positioned in the tubulovesicles in permanent confluence with the $(H^+ + K^+)$-ATPase. In that case, in the light of the result with microsomes, an extrinsic mechanism for conductance repression in the non-secreting state will have to be postulated. Further biochemical studies, in particular the isolation of the apical membrane of the resting cell will serve to clarify this interesting cellular phenomenon.

We wish to thank Dr. Rolf Mehlhorn for his advice and discussion in regards to the EPR studies.

This work was supported in part by a grant from the U.S. Public Health Service, AM 10141.

References

Beauge, L.A., Cavieres, J.J., Glynn, I.M., Grantham, J.J. 1980. The effect of vanadate on the fluxes of sodium and potassium ions through the sodium pump. *J. Physiol. (London)* **301:**7–23

Bernhardt, I., Donath, E., Glaser, R. 1984. Influence of surface charge and transmembrane potential on rubidium-86 efflux of human red blood cells. *J. Membrane Biol.* **78:**249–255

Berry, E.A., Hinkle, P.C. 1983. Measurement of electrochemical proton gradient in submitochondrial particles. *J. Biol. Chem.* **258:**1474–1486

Black, J.A., Forte, T.M., Forte, J.G. 1980. Structure of oxyntic cell membranes during conditions of rest and secretion of HCl as revealed by freeze fracture. *Anat. Rec.* **196:**163–172

Bradford, M.M. 1976. A rapid and sensitive method for the quantitation of microgram quantities of protein utilizing the principle of protein-dye binding. *Anal. Biochem.* **72:**248–254

Bradford, N.M., Davies, R.E. 1950. The site of hydrochloric acid production in the stomach as determined by indicators. *Biochem. J.* **46:**414–420

Culp, D.J., Wolosin, J.M., Soll, A.H., Forte, J.G. 1983. Muscarinic receptors and guanylate cyclase in mammalian gastric glandular cells. *Am. J. Physiol.* **245:***G*760–*G*768

Dawson, R.M.C., Elliot, D.C., Elliot, W.H., Jones, K.M. 1969. Data for Biochemical Research. (2nd Ed.) p. 430. Oxford Press, London

DiBona, R., Ito, S., Berglindh, T., Sachs, G. 1979. Cellular site of gastric acid secretion. Proc. Natl. Acad. Sci. USA **76:**6689–6693

Faller, L.D., Rabon, E., Sachs, G. 1983. Vanadate binding to the gastric H,K-ATPase and inhibition of the enzyme catalytic transport activities. *Biochemistry* **22:**4676–4683

Forte, J.G., Lee, H.C. 1977. Gastric adenosine triphosphatases: A review of their possible role in HCl secretion. *Gastroenterology* **73:**921–926

Forte, T.M., Machen, T.E., Forte, J.G. 1977. Ultrastructural change sin oxyntic cells associated with secretory function: A membrane recycling hypothesis. *Gastroenterology* **73:**941–955

Grinstein, S., Clarke, C.A., Rothstein, A., Gelfand, E.W. 1983. Volume induced anion conductance in human B lymphocytes is cation independent. *Am. J. Physiol.* **245:***C*160–*C*163

Gutknecht, J., Walter, A. 1981. SCN^{-1} and HSCN transport through lipid bilayer membranes, a model for SCN^- inhibition of gastric acid secretion. *Biochim. Biophys. Acta* **685:**233–240

Hoffman, E.K., Simonsen, L.O., Lambert, I.H. 1984. Volume-induced increase of K^+ and Cl^- permeabilities in Ehrlich ascites tumor cells. Role of internal Ca^{2+}. *J. Membrane Biol.* **78:**211–222

Hopfer, U., Liedtke, C.L. 1981. Kinetic features of cotransport mechanisms under isotope exchange conditions. *Memb. Biochem.* **4:**11–29

Houslay, M.D., Stanley, K.K. 1982. Dynamics of Biological Membranes. Chapter 3. John Wiley, New York

Ito, S., Schofield, G.G. 1974. Studies on the depletion and accumulation of microvilli and changes in the tubulovesicular compartment of mouse parietal cells in relation to gastric acid secretion. *J. Cell Biol.* **63:**364–382

Latorre R., Miller, C. 1983. Conduction and selectivity in potassium channels. *J. Membrane Biol.* **71:**11–30

Rabon, E., Takeguchi, N., Sachs, G. 1980. Water and salt permeability of gastric vesicles. *J. Membrane Biol.* **53:**109–117

Reenstra, W.W., Forte, J.G. 1982. Action of thiocyanate on pH gradient formation by gastric microsomal vesicles. *Am. J. Physiol.* **244:***G*308–*G*313

Sachs, G., Chang, H., Rabon, E., Schackmann, R., Lewin, M., Saccomani, G. 1976. A non electrogenic H^+ pump in plasma membrane of hog stomach. *J. Biol. Chem.* **251:**7690–7698

Schackmann, R., Schwartz, A., Saccomani, G., Sachs, G. 1977. Cation transport by gastric $(H^+ + K^+)$-ATPase. *J. Membrane Biol.* **32:**361–381

Smolka, A., Helander, H., Sachs, G. 1983. Monoclonal antibodies against the gastric $(H^+ + K^+)$-ATPase. *Am. J. Physiol.* **245:***G*589–*G*596

Stark, G., Benz, R., Pohl, G.W., Janko, K. 1972. Valinomycin as a probe for the study of structural changes in black lipid membranes. *Biochim. Biophys. Acta* **226:**603–612

Tourtellotte, M.E., Branton, D., Keith, A. 1970. Membrane structure: Spin labeling and freeze etching of *Mycoplasma laidlawi*. *Proc. Natl. Acad. Sci. USA* **66:**909–916

Wolosin, J.M., Forte, J.G. 1981*a*. Changes in the membrane environment of the $(K^+ + H^+)$-ATPase following stimulation of gastric oxyntic cell. *J. Biol. Chem.* **256:**3149–3152

Wolosin, J.M., Forte, J.G. 1981*b*. Functional differences between K^+-ATPase membranes isolated from resting or stimulated rabbit fundic mucosa. *FEBS Lett.* **125:**208–212

Wolosin, J.M., Forte, J.G. 1983. Anion exchange in oxyntic cell apical membrane. Relationship of thiocyanate inhibition of acid secretion. *J. Membrane Biol.* **76:**261–268

Wolosin, J.M., Forte, J.G. 1984. Stimulation of the oxyntic cell triggers K^+ and Cl^- conductances in the apical $(H^+ + K^+)$-ATPase membrane. *Am. J. Physiol.* **246:**C537–C545

Received 8 June 1984; revised 11 September 1984